

Supported by



Accepted Article

Title: Porous FeO(OH) dispersed on Mg-Al hydrotalcite surface for one-pot synthesis of 2-substituted quinoline derivatives

Authors: Ken Motokura, Nao Ozawa, Risako Sato, Yuichi Manaka, and Wang-Jae Chun

This manuscript has been accepted after peer review and appears as an Accepted Article online prior to editing, proofing, and formal publication of the final Version of Record (VoR). This work is currently citable by using the Digital Object Identifier (DOI) given below. The VoR will be published online in Early View as soon as possible and may be different to this Accepted Article as a result of editing. Readers should obtain the VoR from the journal website shown below when it is published to ensure accuracy of information. The authors are responsible for the content of this Accepted Article.

To be cited as: *ChemCatChem* 10.1002/cctc.202100338

Link to VoR: <https://doi.org/10.1002/cctc.202100338>

RESEARCH ARTICLE

Porous FeO(OH) Dispersed on Mg-Al Hydrotalcite Surface for One-Pot Synthesis of Quinoline Derivatives

Ken Motokura,^{*,[a],[b]} Nao Ozawa,^[a] Risako Sato,^[a] Yuichi Manaka,^{[a],[c]} and Wang-Jae Chun^[d]

[a] Prof. K. Motokura, N. Ozawa, R. Sato, Prof. Y. Manaka
Department of Chemical Science and Engineering, School of Materials and Chemical Technology
Tokyo Institute of Technology
4259 Nagatsuta-cho, Midori-ku, Yokohama, 226-8502, Japan
E-mail: motokura.k.ab@m.titech.ac.jp

[b] Prof. K. Motokura
PRESTO, Japan Science and Technology Agency (JST)
4-1-8 Honcho, Kawaguchi, Saitama 332-0012, Japan

[c] Prof. Y. Manaka
Renewable Energy Research Center
National Institute of Advanced Industrial Science and Technology (AIST)
2-2-9 Machiikedai, Koriyama, Fukushima 963-0298, Japan

[d] Prof. W.-J. Chun
Graduate School of Arts and Sciences
International Christian University
Mitaka, Tokyo, 181-8585, Japan

Supporting information for this article is given via a link at the end of the document.

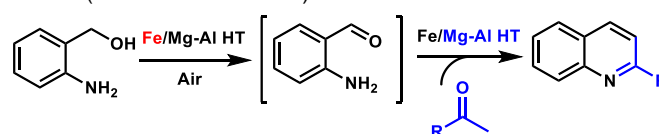
Abstract: The use of ubiquitous elements such as iron instead of expensive precious metals as catalysts is one goal toward realizing environmentally benign synthetic chemistry. Here, we report that porous FeO(OH) dispersed on Mg-Al hydrotalcite acts as a bifunctional heterogeneous catalyst in the one-pot synthesis of 2-substituted quinoline derivatives through dehydrogenative oxidation-cyclization reactions. The catalyst was prepared by a simple grafting method using FeCl₃ and Mg-Al hydrotalcite. The prepared porous FeO(OH) possesses a higher surface area than those previously reported for α-FeO(OH) particles. The one-pot quinoline synthesis proceeded effectively under non-noble-metal catalysis in air without requiring additional homogeneous bases or solvents.

Introduction

Quinoline derivatives are important chemical intermediates in the synthesis of pharmaceuticals.^[1] A general preparation method of 2-substituted quinoline is by using the Friedländer method, which involves a cyclization reaction between 2-aminobenzaldehyde and ketones.^[2] Due to the unstable nature of 2-aminobenzaldehyde, one-pot synthesis of 2-substituted quinolines from 2-aminobenzylalcohol with ketones has been developed using transition metal-inorganic base mixed catalyst systems. In 2001, Cho and co-workers reported RuCl₂(=CHPh)(PCy₃)₂ with KOH for reaction sequences containing dehydrogenation of 2-aminobenzylalcohol followed by cyclization with ketones.³ Not only Ru⁴ but also Ni,⁵ Ir,⁶ Cu,⁷ Mn,⁸ Pd,⁹ and other metals¹⁰ have been used to promote the one-pot synthesis along with additional homogeneous bases.¹¹ The reports on the catalyst system for one-pot quinoline synthesis is summarized in Table S4. Recently, dehydrogenation from alcohol using iron catalysts have received much attention due to the low toxicity and abundance of Fe.¹² Homogeneous and heterogeneous Fe-catalyzed dehydrogenation systems have been applied successfully to quinoline synthesis,^{13,14} however, the

use of homogeneous additives, solvents, and atmospheric remains necessary.

Accumulation of different catalytically active sites on the same solid surface is an effective procedure that can promote multiple processes in a one-pot synthesis. For example, hydrotalcite-supported metal catalysts have been reported as multifunctional catalysts possessing transition metals and/or base sites for several one-pot reactions, including the quinoline synthesis.^{4a,15,16} For example, Mizuno and co-workers demonstrated that hydrotalcite-supported Au nanoparticles can catalyze the one-pot synthesis of flavones through selective dehydrogenation and carbon-carbon bonds forming reactions that are promoted by Au and the basic sites, respectively.¹⁵ These results indicate that hydrotalcite is an ideal material as both a support of transition metal and a solid base and can maintain and/or enhance the catalytic properties of both.¹⁶ Regarding the combination of hydrotalcite and Fe, Kaneda and co-workers reported Mg-Al-Fe type hydrotalcite as an efficient catalyst for the Baeyer-Villiger oxidation of ketones.¹⁷ Additionally, hydrotalcite compounds including Fe species have been frequently used for reduction, oxidation, and electrochemical reactions such as water splitting reactions.^{18,19} This beneficial chemistry between Fe and hydrotalcite encouraged us to investigate the one-pot quinoline synthesis using hydrotalcite-supported iron catalyst (Fe/Mg-Al HT) (Scheme 1). Careful spectroscopic analysis implies that the accumulated Fe species on Mg-Al HT surface was reconstructed to porous FeO(OH), which showed high performance in quinoline synthesis. Some of the advantages of our reaction system are the following: (i) use of a non-noble-metal heterogeneous catalyst, (ii) no need of additional bases and solvents, and (iii) no atmospheric control (reaction occurs in air).



- noble-metal free
- without any additives and solvents
- under Air

RESEARCH ARTICLE

Scheme 1. One-pot quinoline synthesis catalysed by Fe/Mg-Al HT

Results and Discussion

Preparation and Characterization of Catalysts

Mg-Al HT (Mg:Al=3:1) with a carbonate anion ($\text{Al}_2\text{Mg}_6(\text{OH})_{16}\text{CO}_3\cdot 4\text{H}_2\text{O}$) was obtained from Tomita Pharmaceutical Co.. Fe/Mg-Al HT was prepared by a simple impregnation procedure, that is, Mg-Al HT was treated by an aqueous solution of FeCl_3 at room temperature. The resulting slurry was added to sodium hydroxide solutions, filtrated, washed, and dried under vacuum at room temperature, leading to Fe/Mg-Al HT. Hydrotalcite-like compounds containing Fe cation in its brucite layer (Mg-Al-Fe) were synthesized by the co-precipitation method using $\text{MgCl}_2\cdot 6\text{H}_2\text{O}$, $\text{AlCl}_3\cdot 6\text{H}_2\text{O}$, and FeCl_3 . Fe, Mg, and Al contents of Fe/Mg-Al HT and Mg-Al-Fe were determined by ICP analysis, as summarized in Table 1. The loading amount of Fe of Fe/Mg-Al HT was easily controlled in the range of 0.10 to 2.28 mmol g^{-1} . The samples are referred to as Fe(x)/Mg-Al HT or Mg-Al-Fe(x), where x is the loading amount of Fe (mmol g^{-1}). In addition, Fe/Mg-Al HT with a high surface area (Fe/Mg-Al HT[HS]) was also prepared by a similar co-precipitation from MgCl_2 and AlCl_3 , followed by the treatment of the obtained solid with an aqueous FeCl_3 solution.

Fig. 1 shows XRD patterns of the parent Mg-Al HT, Fe(1.4)/Mg-Al HT, and Mg-Al-Fe(1.9). Both Fe-containing samples showed the layered structure of hydrotalcite compounds. No clear signals that could be assigned to iron oxides and hydroxides was detected. Peak positions of Fe/Mg-Al HT were almost the same as those of the support Mg-Al HT. Meanwhile, peak positions of (003) and (006) reflections of Mg-Al-Fe(1.9) shifted slightly (Table S1, Supplementary Information), suggesting the incorporation of Fe cations in the hydrotalcite brucite layer.²⁰

Fe K-edge XAFS measurements were conducted to determine the local structure. The features and edge positions of XANES spectra of Fe/Mg-Al HT and Mg-Al-Fe were close to those of $\text{Fe}(\text{III})_2\text{O}_3$, but differed significantly from those of $\text{Fe}(\text{II})\text{O}$ and Fe foil (Fig. S1, Supplementary Information). The presence of $\text{Fe}(\text{III})$ species in Fe-containing samples can be suggested. The Fe $2p_{3/2}$ signal position of Fe/Mg-Al HT was 710.8 eV in XPS analysis (Figure S10, Supplementary Information). This also supports the presence of Fe^{3+} . Fe K-edge EXAFS spectra are shown in Fig. 2. Interestingly, the spectral features of Fe/Mg-Al HT and Mg-Al-Fe were significantly different. For example, in Mg-Al-Fe, strong peaks and shoulders at 4.4, 5.2, 5.9, 7.5, and 8.1 \AA^{-1} were detected, while no such peaks were observed for Fe/Mg-Al HT. The EXAFS spectrum of Mg-Al-Fe is assignable to Fe cation in the brucite layer of Mg-Fe HT-like compounds.^{18,20} We also prepared the Fe hydroxide-like precipitate from aqueous FeCl_3 and NaOH in the absence of the Mg-Al HT support. The EXAFS spectrum of the Fe hydroxide-like precipitate is shown in Fig. 2 as a black dotted line. The EXAFS spectrum of Fe/Mg-Al HT is similar to that of the Fe hydroxide-like precipitate. This similarity increased with increasing Fe loading on the Mg-Al HT. Wang and co-workers reported the preparation of an $\alpha\text{-FeO}(\text{OH})$ precursor through a similar procedure by using an aqueous FeCl_3 solution with NaOH treatment.²¹ Careful XRD analysis of the Fe hydroxide-like precipitate indicated broad signals at $2\theta=21^\circ$, 36° , and 60° assignable to (110), (130), (111), and (221), (160)

reflections of $\alpha\text{-FeO}(\text{OH})$, respectively (Fig. S2, Supplementary Information). FT of k^3 -weighted Fe K-edge EXAFS (FT-EXAFS) spectrum for Fe-containing samples showed that Fe/Mg-Al HT catalysts lead to strong signals at 1.5 \AA (Fig. S3, Supplementary Information). This signal position is close to that of Fe-O but different from that of Fe-Cl. Curve-fitting analysis of the signal in Fe(1.4)/Mg-Al HT by using the Fe-O parameter was conducted as shown in Table S2, Supplementary Information. The signal for Fe-O was well fitted with a coordination number (N) of approximately 6 and bond length of 2.01 \AA . These results indicate that the local structure of Fe species on Fe/Mg-Al HT surface was similar to that of $\alpha\text{-FeO}(\text{OH})$.

Table 1. Elemental analysis of prepared samples by ICP.

Catalyst	Fe (mmol/g)	Mg (mmol/g)	Al (mmol/g)
Fe(0.1)/Mg-Al HT	0.10	9.3	3.8
Fe(0.5)/Mg-Al HT	0.50	9.4	3.6
Fe(1.4)/Mg-Al HT	1.42	7.4	2.4
Fe(2.3)/Mg-Al HT	2.28	5.7	1.7
Mg-Al-Fe(1.3)	1.25	8.5	2.6
Mg-Al-Fe(1.9)	1.90	7.8	2.4
Fe(1.5)/Mg-Al HT[HS]	1.52	8.7	2.6

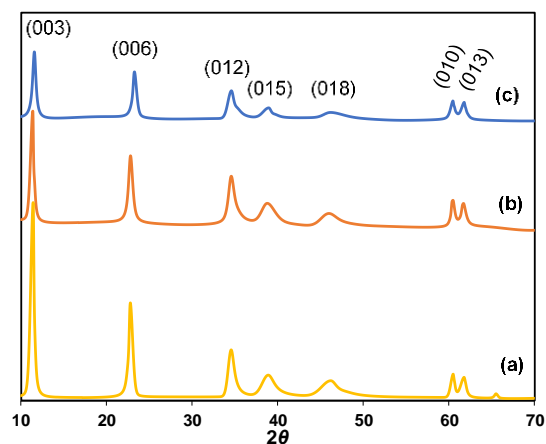
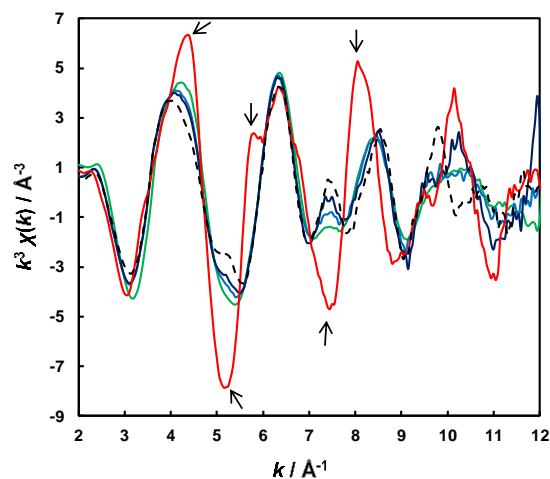


Figure 1. XRD patterns of (a) Mg-Al HT, (b) Fe(1.4)/Mg-Al HT, and (c) Mg-Al-Fe(1.9).



RESEARCH ARTICLE

Figure 2. k^2 -weighted Fe K-edge EXAFS spectra of Fe(2.3)/Mg-Al HT (dark blue), Fe(1.4)/Mg-Al HT (blue), Fe(0.5)/Mg-Al HT (green), Mg-Al-Fe(1.3) (red), and Fe hydroxide precipitate (black, dotted).

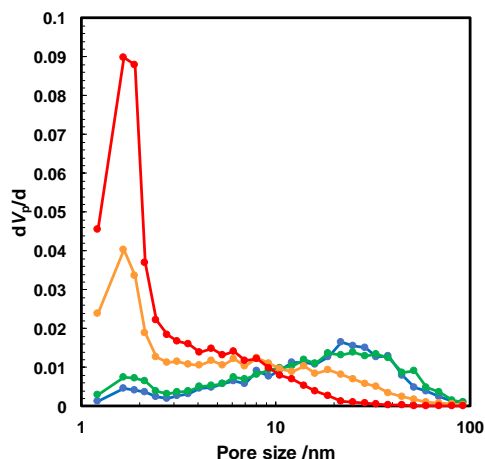


Figure 3. Pore size distribution of the parent Mg-Al HT (blue), Fe(0.1)/Mg-Al HT (green), Fe(1.4)/Mg-Al HT (orange), and Fe(2.3)/Mg-Al HT (red).

Table 2. Surface area and pore volume of samples determined by BET analysis.

Catalyst	Surface area (m^2g^{-1})	Pore volume (cm^3g^{-1})
Mg-Al HT	59	0.65
Fe(0.1)/Mg-Al HT	64	0.69
Fe(1.4)/Mg-Al HT	114	0.40
Fe(2.3)/Mg-Al HT	168	0.26
Mg-Al-Fe(1.3)	131	0.62
Fe(1.5)/Mg-Al HT[HS]	155	0.50

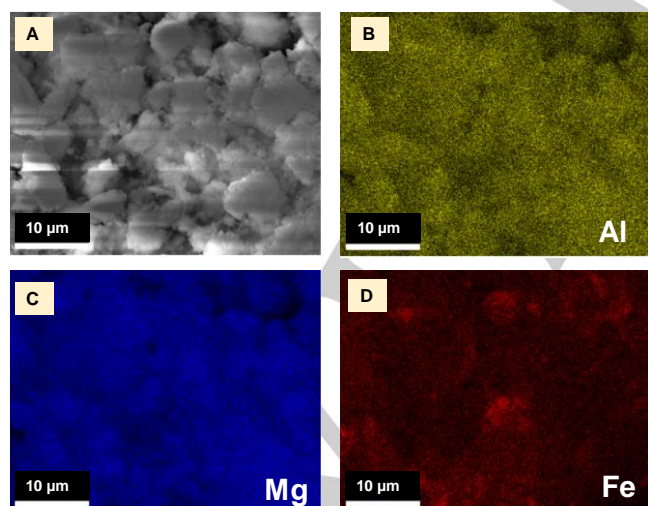


Figure 4. (A) SEM image of Fe(1.4)/Mg-Al HT, EDS mapping results of elements (B) Al, (C) Mg, and (D) Fe. Scale bar = 10 μm .

FT-EXAFS spectra of both the Fe/Mg-Al HT and Fe hydroxide-like precipitate show sharp signals at 1.5 and 2.6 \AA , which can be assigned to Fe-O and Fe-O-Fe, respectively

(Fig. S4); here, the signal intensity of Fe-O-Fe of Fe/Mg-Al HT is weaker than that of the Fe hydroxide-like precipitate, suggesting dispersion of small FeO(OH) clusters on the Mg-Al HT surface. UV-vis spectra of Fe(1.4)/Mg-Al HT show a broad band around 300-400 nm and 500 nm, assignable to oligomeric Fe clusters and aggregated Fe species, respectively (Fig. S5).^{18,22} Fig. 3 shows the pore size distribution of the parent Mg-Al HT and Fe/Mg-Al HT with different Fe loadings. Interestingly, with increasing Fe loading, pores with a diameter of 1.7 nm increased significantly, whereas pores with diameters in the range 20-30 nm derived from hydrotalcite support surface decreased. The surface area also increased with Fe loading (Table 2). SEM-EDS analysis of Fe(1.4)/Mg-Al HT indicates dispersion of Fe species on the Mg-Al HT surface (Fig. 4). These characterizations imply that the Mg-Al HT surface was decorated by highly dispersed porous FeO(OH) clusters. Guo and co-workers reported porous α -FeO(OH) prepared in alkaline media from a $\text{Fe}(\text{NO}_3)_3$ solution with a surface area of $46\text{ m}^2\text{g}^{-1}$.²³ Meanwhile, as shown in Table 2, the surface area increased from 58.6 to $114\text{ m}^2\text{g}^{-1}$ for Fe(1.4)/Mg-Al HT after Fe loading. Since the parent Mg-Al HT has a surface area of only $59\text{ m}^2\text{g}^{-1}$, the surface area derived from the porous FeO(OH) particle attached on the HT surface can be simply calculated to be $440\text{ m}^2\text{g}^{-1}$ using its Fe content (7.9 wt%). This calculation is based on the hypothesis of the simple mixture of Mg-Al HT and Fe compound because of the maintenance of Mg-Al HT structure and oligomeric/aggregated form of surface Fe species. Dispersion of porous FeO(OH) particles on the Mg-Al HT surface maintains their high surface area.

One-pot synthesis of quinolines

Quinoline synthesis from 2-aminobenzyl alcohol (**1**) contains two reaction steps: (i) oxidative dehydrogenation of alcohol to aldehyde and (ii) base-catalyzed cyclization reaction between 2-aminobenzaldehyde and carbonyl compounds.²⁻¹⁰ The reaction between **1** and acetophenone (**2a**) was investigated using HT-supported Fe catalysts at $100\text{ }^\circ\text{C}$ under air (Fig. 5). On increasing the Fe loading, conversion of **1** increased. Regarding 2-phenylquinoline (**3a**) productivity, Fe(1.4)/Mg-Al HT showed a slightly higher yield than that given by Fe(2.3)/Mg-Al HT. These results indicate that the Fe site accelerates the dehydrogenation of **1**, while the basicity of Mg-Al HT support is not strongly deactivated by the Fe species on the surface. In the case of Mg-Al-Fe, both conversion and yield decreased when compared with Fe(1.4)/Mg-Al HT even with a similar loading of Fe as well as a surface area (Table 2); this could be due to the accessibility of the Fe site.

To increase the quinoline yield, the reaction was conducted at $150\text{ }^\circ\text{C}$. The results are summarized in Table 3. A 89% yield of **3a** was obtained with Fe(1.4)/Mg-Al HT after 24 h. Catalytic activity of Fe/Mg-Al HT depends on the surface area, that is, when Fe(1.5)/Mg-Al HT[HS] was used, the product yield slightly increased to 91%. Other magnesium and aluminum oxide and hydroxide supports did

RESEARCH ARTICLE

not show good performance. For example, the yield decreased to 8% when using Fe/Al₂O₃. The yield was still 59% even after the addition of 0.25 g of the Mg-Al HT to the reaction mixture. Not only the dehydrogenation, but also the base-catalyzed cyclization ability was lower in the case of other supports. Fe compounds, such as Fe₂O₃ and FeCl₃, were almost inactive for the quinoline production. Other metal on Mg-Al HT also showed activity for the quinoline synthesis. HT with Mn and Cu species that previously reported highly active combinations for the dehydrogenation of alcohol,²⁴ also showed good performance for the quinoline production.

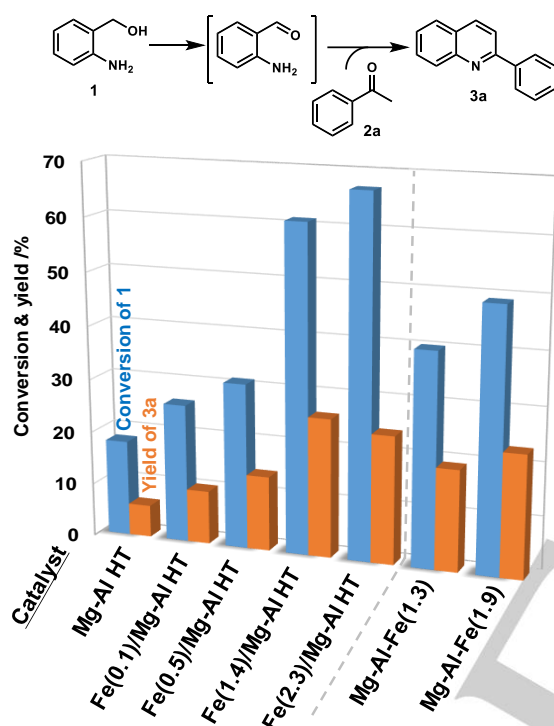


Figure 5. One-pot synthesis of **3a** from **1** and **2a** using supported Fe catalysts. Reaction conditions: **1** (1.0 mmol), **2a** (4.8 mmol), catalyst (0.25 g), neat, 100 °C, 24 h, Air.

Table 3. One-pot synthesis of **3a** from **1** and **2a** using various catalyst^a

Catalyst	Conv. of 1 (%) ^b	Yield of 3a (%) ^b
Fe(0.5)/Mg-Al HT	99	79
Fe(1.4)/Mg-Al HT	99	89 (67 ^e , 61 ^f)
Fe(1.5)/Mg-Al HT[HS]	99	91
Mg-Al-Fe(1.3)	99	83
Mg-Al-Fe(1.9)	99	83
Fe/Mg(OH) ₂	80	36
Fe/MgO	39	12
Fe/Al ₂ O ₃	93	8
Fe/Al ₂ O ₃ + Mg-Al HT ^c	95	59
α-FeO(OH)	98	8
α-Fe ₂ O ₃	92	12
FeO	74	5

FeCl ₃ ^d	99	<1
Mn/Mg-Al HT	99	90
Cu/Mg-Al HT	99	90
Co/Mg-Al HT	99	51
Ni/Mg-Al HT	90	43
Mg-Al HT	96	65
none	55	2

^a Reaction conditions: **1** (1.0 mmol), **2a** (4.8 mmol), catalyst (0.25 g), neat, 150 °C, 24 h, Air. ^bDetermined by ¹H NMR. ^c0.25 g of HT was added. ^d0.125 mmol was used. Fe loading: Fe/Mg(OH)₂: 0.49 mmol g⁻¹; Fe/MgO 0.44 mmol g⁻¹; Fe/Al₂O₃: 0.46 mmol g⁻¹. ^e2nd use. ^f3rd use.

The scope of the substrate applicability is summarized in Table 4. Fe/Mg-Al HT showed wide applicability toward various ketones for the one-pot quinoline synthesis. Various substitution groups could be introduced to acetophenone, affording good to excellent yields of the corresponding product. Other functionalities such as naphthyl and heteroaromatic groups were applicable: for example, the reaction of 2-acetylpyridine resulted in 83% yield of the quinoline product. This result indicates that the Fe/Mg-Al HT is not deactivated by the coordination of bipyridine derivatives. Ketones with substitution group on the α-position, α-tetralone and propiophenone, were also acted as good substrate to give 2,3-disubstituted quinolines. After the reaction, the catalyst was recovered and reused for a second time. Unfortunately, the catalytic activity dropped to 38% after simple washing of recovered catalyst by diethyl ether, while Fe K-edge XAFS analysis of the recovered catalyst did not show any change in the Fe local structure and layered

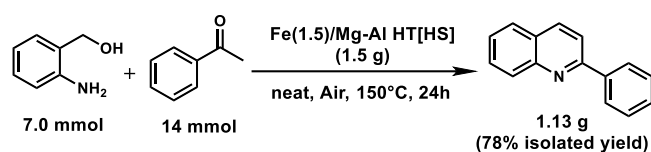
Table 4 Scope of ketones for one-pot quinoline synthesis^a

91%*	84%	76%
73%	81%*	84%*
83%*	75%*, ^b	83%
66%*	71%*	81%*
69%*	73%*	

RESEARCH ARTICLE

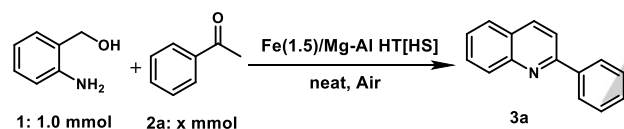
^a Reaction conditions: **1** (1.0 mmol), ketone (4.8 mmol), Fe(1.4)/Mg-Al HT (0.25 g), neat, 150 °C, 24 h, Air. ¹H NMR Yield. *Fe(1.5)/Mg-Al HT[HS] was used. ^b 48 h.

structure of HT support (Table S3, Figure S6 and S11, Supporting Information). Therefore, to reactivate the basic site of Fe/Mg-Al HT, the recovered catalyst was treated by an aqueous NaOH solution, resulting in quinoline yields of 67% (2nd use) and 61% (3rd use) (Table 3 and S3). The reactivation process does not affect the Fe local structure (Fig. S6), suggesting reactivation of surface base site. To achieve a yield higher than 90%, 4.8 equivalents of **3a** was necessary. However, good to acceptable yields were observed with a decreases in the amount of **2a** (Table 5). The reaction also proceeded well with 0.86 g of **1** with 2 equivalents of **2a** on using Fe(1.5)/Mg-Al HT[HS], giving 1.13 g of **3a** with 78% isolated yield (Scheme 2).



Scheme 2 Gram-scale synthesis of **3a**

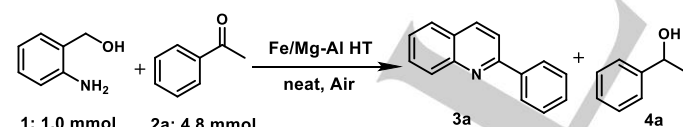
Table 5. Effect of **2a** amount on the one-pot quinoline synthesis ^a



x (2a mmol)	Conv. of 1 (%)	Yield of 3a (mmol)
4.8	>99	91
2.0	>99	87
1.5	>99	72

^a Reaction conditions: **1** (1.0 mmol), **2a** (x mmol), Fe(1.5)/Mg-Al HT[HS] (0.25 g), neat, 24 h, Air.

Table 6. Effect of Fe loading on the one-pot quinoline synthesis ^a



Catalyst	Temp. (°C)	Yield of 3a (mmol)	Yield of 4a (mmol)
Fe(0.5)/Mg-Al HT	150	0.79	0.53
Fe(1.4)/Mg-Al HT	150	0.89	0.10
Fe(0.5)/Mg-Al HT	100	0.14	0.05
Fe(1.4)/Mg-Al HT	100	0.26	0.05

^a Reaction conditions: **1** (1.0 mmol), **2a** (4.8 mmol), catalyst (0.25 g), neat, 24 h, Air.

To confirm the heterogeneity of the catalyst, hot filtration test was performed. The catalyst (Fe(1.4)/Mg-Al HT) was filtrated at ca. 30% yield of 2-phenylquinoline, and the filtrate was heated for 24 h. After 24 h, the product yield was ~35%, while the yield achieved to 89% without the filtration of Fe(1.4)/Mg-Al HT catalyst. These results clearly indicate that the reaction occurs on the surface of the catalyst.

To understand the reaction pathway, the effect of Fe loading on the catalysis was analyzed in detail. In the case of Fe(0.5)/Mg-Al HT, 0.53 mmol of 1-phenylethanol (**4a**) was formed along with 0.79 mmol of **3a** at 150 °C, while the amount of **4a** was only 0.10 mmol with 0.89 mmol of **3a** using Fe(1.4)/Mg-Al HT (Table 6). This result indicates that Meerwein-Ponndorf-Verley (MPV)-type hydrogen transfer reaction mainly occurs for a catalyst with low Fe loading, while aerobic oxidation of **1** preferentially occurs at the Fe site. Meanwhile, when the reaction is conducted at 100 °C, the amount of **4a** was much lower than the amount of **3a** and converted **1** (Table 6 and Fig. 5). This result suggests that the MPV hydrogen transfer reaction scarcely occurs at 100 °C. To further understand the effect of O₂, the reaction was conducted under Ar at 100 °C. The reaction under Ar gave a similar initial reaction rate as that in air (N₂ and O₂); however, after 24 h, the conversion of **1** in air and Ar was 67 and 33%, respectively (Fig. S9, Supplementary Information). This result indicates that molecular oxygen was consumed in the dehydrogenative oxidation of **1**, while stoichiometric oxidation reaction on the surface FeO(OH) species occurred without O₂. The addition of the radical trap, 2,3-di-tert-butyl-p-cresol had little influence on the conversion rate of **1**. The reaction of cyclopropyl methyl ketone proceeded to give the corresponding product without skeletal isomerization or C-C bond cleavage (Table 4). Although the detailed mechanism is still unclear, nonradical oxidation of alcohol **1** on an active Fe-O(H) species^[25] followed by a re-activation of the Fe site by O₂ can be proposed as a possible mechanism. As mentioned above, the simple addition of Mg-Al HT to a Fe catalyst accelerates **3a** formation (Table 3). The aldehyde intermediate reacts with a ketone to give 2-substituted quinoline products at the basic site on Mg-Al HT.

Conclusion

A novel porous FeO(OH) was prepared on the Mg-Al HT surface with a high surface area. The prepared supported catalyst showed a high performance in one-pot quinoline synthesis through aerobic oxidation of alcohol and cyclization between an aldehyde and ketone at the active Fe species and at the basic site on the HT surface, respectively. The non-noble-metal, heterogeneous, and additive- and solvent-free reaction system provides a pathway to environmentally-benign synthetic protocols.

Acknowledgements

This study was supported by a JSPS Grant-in-Aid for Scientific Research on Innovative Areas (grant no. 20H04804), the Tokuyama Science Foundation, the Innovative Research Initiative project in Tokyo Tech, and the AIST-Tokyo Tech cross-appointment system.

Keywords: Iron Catalyst • Hydrotalcite • Quinoline • One-pot Synthesis

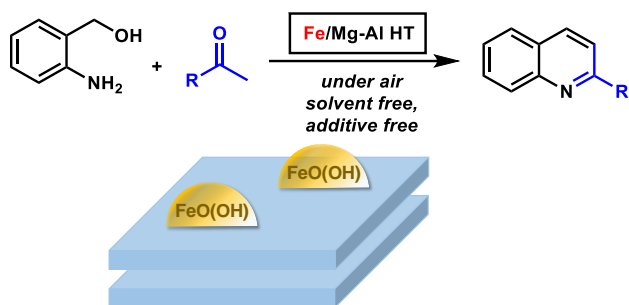
- [1] (a) G. R. Newkome and W. W. Paudler, *Contemporary Heterocyclic Chemistry*, Wiley, New York, 1982; pp 199-231. (b) A. R. Katritzky, *Handbook of Heterocyclic Chemistry*, Pergamon Press: Oxford, U.K., 1985.

RESEARCH ARTICLE

- [2] J. Marco-Contelles, E. Pérez-Mayoral, A. Samadi, M. C. Carreiras and E. Soriano, *Chem. Rev.* **2009**, *109*, 2652-2671.
- [3] C. S. Cho, B. T. Kim, T.-J. Kim and S. C. Shim, *Chem. Commun.* **2001**, 2576-2577.
- [4] (a) K. Motokura, T. Mizugaki, K. Ebitani and K. Kaneda, *Tetrahedron Lett.* **2004**, *45*, 6029-6032; (b) R. Martínez, G. J. Brand, D. J. Ramón and M. Yus, *Tetrahedron Lett.* **2005**, *46*, 3683-3686; (c) R. Martínez, D. J. Ramón and M. Yus, *Tetrahedron* **2006**, *62*, 8988-9001; (d) H. Vander Mierde, N. Ledoux, B. Allaert, P. Van Der Voort, R. Drozdak, D. De Vos, and F. Verpoort, *New J. Chem.* **2007**, *31*, 1572; (e) H. Vander Mierde, P. Van Der Voort, D. De Vos and F. Verpoort, *Eur. J. Org. Chem.* **2008**, *9*, 1625-1631; (f) M. Subramanian, S. Sundar and R. Rengan, *Appl. Organomet. Chem.* **2018**, *32*, e4582; (g) G. Balamurugan, S. Balaji, R. Ramesh and N. S. P. Bhuvanesh, *Appl. Organomet. Chem.* **2019**, *33*, e4696; (h) B. Guo, T. Q. Yu, H. X. Li, S. Q. Zhang, P. Braunstein, D. J. Young, H. Y. Li and J. P. Lang, *ChemCatChem* **2019**, *11*, 2500-2510; (i) S. N. R. Donthireddy, P. Mathoor Illam and A. Rit, *Inorg. Chem.* **2020**, *59*, 1835-1847.
- [5] (a) S. Das, D. Maiti and S. De Sarkar, *J. Org. Chem.* **2018**, *83*, 2309-2316; (b) S. Parua, R. Sikari, S. Sinha, S. Das, G. Chakraborty and N. D. Paul, *Org. Biomol. Chem.* **2018**, *16*, 274-284; (c) K. Singh, M. Vellakkaran and D. Banerjee, *Green Chem.* **2018**, *20*, 2250-2256; (d) G. Chakraborty, R. Sikari, S. Das, R. Mondal, S. Sinha, S. Banerjee and N. D. Paul, *J. Org. Chem.* **2019**, *84*, 2626-2641; (e) J. Das, M. Vellakkaran and D. Banerjee, *J. Org. Chem.* **2019**, *84*, 769-779.
- [6] (a) K. Taguchi, S. Sakaguchi and Y. Ishii, *Tetrahedron Lett.* **2005**, *46*, 4539-4542; (b) R. Wang, H. Fan, W. Zhao and F. Li, *Org. Lett.* **2016**, *18*, 3558-61; (c) S. Genc, B. Arslan, S. Gulcemal, S. Gunnaz, B. Cetinkaya and D. Gulcemal, *J. Org. Chem.* **2019**, *84*, 6286-6297; (d) M. Maji, K. Chakrabarti, D. Panja and S. Kundu, *J. Catal.* **2019**, *373*, 93-102; (e) W. Yao, C. Ge, Y. Zhang, X. F. Xia, L. Wang and D. Wang, *Chem. Eur. J.* **2019**, *25*, 16099-16105.
- [7] (a) C. S. Cho, W. X. Ren and S. C. Shim, *Tetrahedron Lett.* **2006**, *47*, 6781-6785; (b) C. S. Cho, W. X. Ren and N. S. Yoon, *J. Mol. Catal. A: Chem.* **2009**, *299*, 117-120; (c) N. T. S. Phan, T. T. Nguyen, K. D. Nguyen and A. X. T. Vo, *Appl. Catal. A: General* **2013**, *464-465*, 128-135; (d) S. Das, S. Sinha, D. Samanta, R. Mondal, G. Chakraborty, P. Brandao and N. D. Paul, *J. Org. Chem.* **2019**, *84*, 10160-10171; (e) S. Elavarasan, A. Bhaumik and M. Sasidharan, *ChemCatChem* **2019**, *11*, 4340-4350; (f) J. Xu, Q. Chen, Z. Luo, X. Tang and J. Zhao, *RSC Adv.* **2019**, *9*, 28764-28767.
- [8] (a) M. K. Barman, A. Jana and B. Maji, *Adv. Synth. Catal.* **2018**, *360*, 3233-3238; (b) X. B. Lan, Z. Ye, M. Huang, J. Liu, Y. Liu, Z. Ke, *Org. Lett.* **2019**, *21*, 8065-8070; (c) C. Zhang, B. Hu, D. Chen and H. Xia, *Organometallics* **2019**, *38*, 3218-3226; for quinazoline synthesis, see: (c) A. Mondal, M. K. Sahoo, M. Subramanian, E. Balaraman, *J. Org. Chem.* **2020**, *85*, 7181-7191.
- [9] (a) C. S. Cho and W. X. Ren, *J. Organomet. Chem.* **2007**, *692*, 4182-4186; (b) R. Mamidala, S. Samsar, N. Sharma, U. Lourderaj and K. Venkatasubbaiah, *Organometallics* **2017**, *36*, 3343-3351.
- [10] (a) G. Zhang, J. Wu, H. Zeng, S. Zhang, Z. Yin and S. Zheng, *Org. Lett.* **2017**, *19*, 1080-1083; (b) D. Wei, V. Dorcet, C. Darcel, J. B. Sortais, *ChemSusChem* **2019**, *12*, 3078-3082; (c) H. J. Seok and C. Shim, *J. Heterocyclic Chem.* **2005**, *42*, 1219-1222.
- [11] Homogeneous strong base has been reported as a catalyst: (a) H. V. Mierde, P. V. D. Voort and F. Verpoort, *Tetrahedron Lett.* **2008**, *49*, 6893-6895; (b) Y.-F. Liang, X.-F. Zhou, S.-Y. Tang, Y.-B. Huang, Y.-S. Feng and H.-J. Xu, *RSC Adv.* **2013**, *3*, 7739; (c) Y. Zhu and C. Cai, *RSC Adv.* **2014**, *4*, 52911-52914; (d) S. Yao, K. Zhou, J. Wang, H. Cao, L. Yu, J. Wu, P. Qiu and Q. Xu, *Green Chem.* **2017**, *19*, 2945-2951.
- [12] (a) B. Join, K. Möller, C. Ziebart, K. Schröder, D. Gördes, K. Thurow, A. Spannenberg, K. Jung and M. Beller, *Adv. Synth. Catal.* **2011**, *353*, 3023-3030; (b) E. Balaraman, A. Nandakumar, G. Jaiswal and M. K. Sahoo, *Catal. Sci. Technol.* **2017**, *7*, 3177-3195; (c) B. Das, M. J. Baruah, M. Sharma, B. Sarma, G. V. Karunakar, L. Satyanarayana, S. Roy, P. K. Bhattacharyya, K. K. Borah and K. K. Bania, *Appl. Catal. A: General* **2020**, *589*, 117292; (d) V. Folliard, G. Postole, L. Marra, J.-L. Dubois and A. Auroux, *Catal. Sci. Technol.* **2020**, *10*, 1889-1901; (e) Y. Gu, P. Lu, W. Zhan, Y. Zhang, L. Sun, G. Chen and Z. Long, *J. Porous Mater.* **2020**, *27*, 701-705; (f) G. Jaiswal, V. G. Landge, D. Jagadeesan and E. Balaraman, *Nat. Commun.* **2017**, *8*, 2147; (g) X. Jiang, J. Zhang and S. Ma, *J. Am. Chem. Soc.* **2016**, *138*, 8344-8347; (h) P. G. Mingalev and G. V. Lisichkin, *Petrol. Chem.* **2020**, *60*, 310-315; (i) F. Shi, M. K. Tse, Z. Li, Z. and M. Beller, *Chem. Eur. J.* **2008**, *14*, 8793-8797.
- [13] S. Elangovan, J. B. Sortais, M. Beller and C. Darcel, *Angew. Chem. Int. Ed.* **2015**, *54*, 14483-6.
- [14] M. Nallagangula, C. Sujatha, V. T. Bhat and K. Namitharan, *Chem. Commun.* **2019**, *55*, 8490-8493.
- [15] T. Yatabe, X. Jin, K. Yamaguchi and N. Mizuno, *Angew. Chem. Int. Ed.* **2015**, *54*, 13302-13306.
- [16] (a) K. Kaneda and T. Mizugaki, *Green Chem.* **2019**, *21*, 1361-1389; (b) S. Nishimura, A. Takagaki and K. Ebitani, *Green Chem.* **2013**, *15*, 2026; (c) K. Motokura, D. Nishimura, K. Mori, T. Mizugaki, K. Ebitani and K. Kaneda, *J. Am. Chem. Soc.* **2004**, *126*, 5662-5663; (d) K. Motokura, N. Fujita, K. Mori, T. Mizugaki, K. Ebitani, K. Jitsukawa and K. Kaneda, *Chem. Eur. J.* **2006**, *12*, 8228-8239; (e) K. Motokura, N. Hashimoto, T. Hara, T. Mitsudome, T. Mizugaki, K. Jitsukawa and K. Kaneda, *Green Chem.* **2011**, *13*, 2416-2422; (f) B. M. Choudary, N. S. Chowdari, S. Madhi and M. L. Kantam, *J. Org. Chem.* **2003**, *68*, 1736-1746.
- [17] K. Kaneda, S. Ueno and T. Imanaka, *J. Mol. Catal. A: Chem.* **1995**, *102*, 135-138.
- [18] T. Kawabata, N. Fujisaki, T. Shishido, K. Nomura, T. Sano and K. Takehira, *J. Mol. Catal. A: Chem.* **2006**, *253*, 279-289.
- [19] (a) V. H. Jadhav, D. K. Dumbre, V. B. Phapale, H. B. Borate and R. D. Wakharkar, *Catal. Commun.* **2007**, *8*, 65-68; (b) D. Kishore and A. E. Rodrigues, *Appl. Catal. A: General* **2008**, *345*, 104-111; (c) Q. Shi, R. Lu, L. Lu, X. Fu and D. Zhao, *Adv. Synth. Catal.* **2007**, *349*, 1877-1881; (d) V. R. Choudhary, D. K. Dumbre, P. N. Yadav and S. K. Bhargava, *Catal. Commun.* **2012**, *29*, 132-136; (e) D. K. Dumbre, T. Mozammel, P. Selvakannan, S. B. Hamid, V. R. Choudhary and S. K. Bhargava, *J. Colloid Interface Sci.* **2015**, *441*, 52-58; (f) Y. Vlamidis, S. Fiorilli, M. Giorgetti, I. Gualandi, E. Scavetta and D. Tonelli, *RSC Adv.* **2016**, *6*, 110976-110985; (g) N. T. Nivangune, V. V. Ranade and A. A. Kelkar, *Catal. Lett.* **2017**, *147*, 2558-2569; (h) W.-J. Liu, L. Dang, Z. Xu, H.-Q. Yu, S. Jin, G. W. Huber, *ACS Catal.* **2018**, *8*, 5533-5541; (i) W. S. Putro, T. Kojima, T. Hara, N. Ichikuni and S. Shimazu, *Catal. Sci. Technol.* **2018**, *8*, 3010-3014; (j) N. Todoroki and T. Wadayama, *ACS Appl. Mater. Interfaces* **2019**, *11*, 44161-44169; (k) X. Zhang, A. N. Marianov, Y. Jiang, C. Cazorla and D. Chu, *ACS Appl. Nano Mater.* **2019**, *3*, 887-895; (l) C. Kuai, Y. Zhang, D. Wu, D. Sokaras, L. Mu, S. Spence, D. Nordlund, F. Lin and X.-W. Du, *ACS Catal.* **2019**, *9*, 6027-6032; (m) D. Yue, X. Yan, C. Guo, X. Qian and Y. Zhao, *J. Phys. Chem. Lett.* **2020**, *11*, 968-973; (n) B. Zhang, C. Zhu, Z. Wu, E. Stavitski, Y. H. Lui, T. H. Kim, H. Liu, L. Huang, X. Luan, L. Zhou, K. Jiang, W. Huang, S. Hu, H. Wang and J. S. Francisco, *Nano Lett.* **2020**, *20*, 136-144; (o) S. Lee, L. Bai and X. Hu, *Angew. Chem. Int. Ed.* **2020**, *59*, 8072-8077.
- [20] M. Vucelic, W. Jones and G. D. Moggridge, *Clays Clay Miner.* **1997**, *45*, 803-813.
- [21] C. Wang, A. Li and C. Shuang, *J. Environment. Management* **2018**, *228*, 158-164.
- [22] G. Centi and F. Vazzana, *F. Catal. Today* **1999**, *53*, 683-693.
- [23] N. Guo, X. Lv, Q. Li, T. Ren, H. Song, Q. Yang, *Microporous Mesoporous Mater.* **2020**, *299*, 110101.
- [24] (a) K. Nagashima, T. Mitsudome, T. Mizugaki, K. Jitsukawa and K. Kaneda, *Green Chem.* **2010**, *12*, 2142-2144; (b) T. Mitsudome, Y. Mikami, K. Ebata, T. Mizugaki, K. Jitsukawa and K. Kaneda, *Chem. Commun.* **2008**, 4804-4806.
- [25] (a) K. Yoshizawa, *Acc. Chem. Res.* **2006**, *39*, 375-382; (b) B. Join, K. Möller, C. Ziebart, K. Schröder, D. Gördes, K. Thurow, A. Spannenberg, K. Junge and M. Beller, *Adv. Synth. Catal.* **2011**, *252*, 3023; (c) F. Shi, M. K. Tse, Z. Li, M. Beller, *Chem. Eur. J.* **2008**, *14*, 8793-8797.

RESEARCH ARTICLE

Entry for the Table of Contents



Porous FeO(OH) dispersed on Mg-Al hydrotalcite acts as a bifunctional heterogeneous catalyst for the one-pot synthesis of quinolines through dehydrogenative oxidation-cyclization reactions. The high surface area of Fe species and strong basicity of hydrotalcite surface enable efficient production of various 2-substituted quinoline derivatives in high yields.